



PII S0016-7037(96)00052-X

Kinetic and mineralogic controls on the evolution of groundwater chemistry and $^{87}\text{Sr}/^{86}\text{Sr}$ in a sandy silicate aquifer, northern Wisconsin, USA

THOMAS D. BULLEN,¹ DAVID P. KRABBENHOFT,² and CAROL KENDALL¹¹Water Resources Division, U.S. Geological Survey, Menlo Park, CA 94025, USA²Water Resources Division, U.S. Geological Survey, Madison, WI 53719, USA

(Received May 24, 1995; accepted in revised form February 8, 1996)

Abstract—Substantial flowpath-related variability of $^{87}\text{Sr}/^{86}\text{Sr}$ is observed in groundwaters collected from the Trout Lake watershed of northern Wisconsin. In the extensive shallow aquifer composed of sandy glacial outwash, groundwater is recharged either by seepage from lakes or by precipitation that infiltrates the inter-lake uplands. $^{87}\text{Sr}/^{86}\text{Sr}$ of groundwater derived mainly as seepage from a precipitation-dominated lake near the head of the watershed decreases with progressive water chemical evolution along its flowpath due primarily to enhanced dissolution of relatively unradiogenic plagioclase. In contrast, $^{87}\text{Sr}/^{86}\text{Sr}$ of groundwater derived mainly from precipitation that infiltrates upland areas is substantially greater than that of precipitation collected from the watershed, due to suppression of plagioclase dissolution together with preferential leaching of Sr from radiogenic phases such as K-feldspar and biotite.

The results of a column experiment that simulated the effects of changing residence time of water in the aquifer sand indicate that mobile waters obtain relatively unradiogenic Sr, whereas stagnant waters obtain relatively radiogenic Sr. Nearly the entire range of strontium-isotope composition observed in groundwaters from the watershed was measured in the experimental product waters. The constant mobility of water along groundwater recharge flowpaths emanating from the lakes promotes the dissolution of relatively unradiogenic plagioclase, perhaps due to effective dispersal of clay mineral nuclei resulting from dissolution reactions. In contrast, episodic stagnation in the unsaturated zone along the upland recharge flowpaths suppresses plagioclase dissolution, perhaps due to accumulation of clay mineral nuclei on its reactive surfaces. Differences in redox conditions along these contrasting flowpaths probably enhance the observed differences in strontium isotope behavior. This study demonstrates that factors other than the calculated state of mineral saturation must be considered when attempting to simulate chemical evolution along flowpaths, and that reaction models must be able to incorporate changing contributions from reacting minerals in the calculations.

1. INTRODUCTION

A major goal of watershed research is to quantify contributions of both water and solutes from different flowpaths to streamflow and lakes. To a first approximation, two contrasting groundwater flowpaths can be envisioned for most watersheds: those dominated by precipitation that originate in, and thus have important contributions from the unsaturated zone; and plumes derived from upgradient surface water bodies such as seepage lakes. Chemical evolution, and thus any unique chemical signature developed along these flowpaths, will vary depending on a variety of factors such as fluid residence time and mobility, flowpath tortuosity, starting water composition, and differences in distributions and reactivities of individual minerals.

Whereas the relative contributions of water from contrasting flowpaths can be determined using the stable water isotope (i.e., hydrogen and oxygen) mass balance method (e.g., Dincer, 1968; Turner et al., 1984; Krabbenhoft et al., 1990), attempts at solute source identification are typically frustrated by the nonconservative nature of most solutes. In a lake, for example, processes such as mixing of two chemically-distinct water types at the lake-groundwater interface or biologic activity in the water column may lead to precipitation of minerals that modify the water composition and thus complicate the recognition of groundwater flow-

path-specific chemical signatures. Clearly, a diagnostic tracer that is unaffected by loss from solution is required for distinguishing solute contributions from divergent groundwater flowpaths.

The naturally occurring isotopes of Sr provide such a tracer. The power of the strontium isotopes lies in the fact that removal of Sr from water as a result of mineral precipitation or cation exchange does not change the isotopic composition of dissolved Sr. Furthermore, although ^{87}Sr is radiogenic (produced by β -decay from ^{87}Rb), the roughly forty-seven billion year half-life of the decay process is so long that on the timescale of groundwater evolution, $^{87}\text{Sr}/^{86}\text{Sr}$ of Sr sources is essentially stable. Long-lived differences in the concentration ratio of Rb to Sr in aquifer minerals lead to significant differences in their relative proportions of radiogenic ^{87}Sr , and thus in the measured value of $^{87}\text{Sr}/^{86}\text{Sr}$. As a Sr-bearing mineral reacts along a groundwater flowpath, Sr having $^{87}\text{Sr}/^{86}\text{Sr}$ of that mineral is dissolved by the water. In theory, groundwaters along various flowpaths can obtain different $^{87}\text{Sr}/^{86}\text{Sr}$ due to the same factors listed above that control chemical evolution.

Our ability to use strontium isotopes to identify solute sources and constrain reaction kinetics along flowpaths requires that the different reactive minerals have distinguishable values or ranges of $^{87}\text{Sr}/^{86}\text{Sr}$. Numerous Rb-Sr geochro-

nologic studies of Precambrian granitic and metamorphic rocks (e.g., references in Faure, 1986) have shown that Rb/Sr and $^{87}\text{Sr}/^{86}\text{Sr}$ of minerals from a single rock are distinctive and typically increase in the order plagioclase, diopside/hornblende, K-feldspar, and mica. Differences in $^{87}\text{Sr}/^{86}\text{Sr}$ among minerals in a sedimentary deposit further depend on factors such as the lithologic diversity and age of the sediment sources. Because the minerals are derived from multiple lithologies, distinctions among minerals will be blurred, but on average differences should persist. At worst, it may not be possible to distinguish between plagioclase and diopside/hornblende, but K-feldspar and especially mica should remain distinctive.

A number of hydrologic studies have exploited the large differences in $^{87}\text{Sr}/^{86}\text{Sr}$ among rocks and their mineral phases to identify solute sources. An important use of strontium isotopes has been to estimate the relative contributions of carbonate and silicate lithologies to water chemistry in a variety of hydrogeologic settings (Fisher and Stueber, 1976; Chaudhuri et al., 1983; Wadleigh et al., 1985; Stueber et al., 1992; Johnson and DePaolo, 1994). At the watershed scale, several studies have used strontium isotopes to determine the relative contributions of various cation sources (i.e., mineral weathering, biomass, dry deposition, precipitation) to stream chemistry, the cation exchange pool or ecosystems (Graustein and Armstrong, 1983; Gosz and Moore, 1989; Aberg et al., 1989; Jacks et al., 1989; Graustein, 1990; Miller et al., 1993; Bailey et al., 1996).

In the watershed studies, the observations that each source may be characterized by a distinct range of $^{87}\text{Sr}/^{86}\text{Sr}$, and that different soil horizons may have isotopically-unique leachable Sr are especially pertinent to this work. In these studies, the isotopic composition of Sr presumed to be provided by weathering has been determined on either weak-acid leachates or total digests of the materials, or by mass-balance calculations that relate residuum to regolith. Cation budget calculations are then typically made using a single average $^{87}\text{Sr}/^{86}\text{Sr}$ as the weathering input to the system. However, Bullen et al. (1996) have cautioned that Sr may be preferentially mobilized from the lattices of presumably resistant minerals such as K-feldspar and hydrobiotite, and thus weathering contributions may not be directly interpretable in terms of strontium isotope variations.

The Trout Lake watershed in the Northern Temperate Lakes region of north-central Wisconsin (Fig. 1) provides an ideal setting to investigate the factors controlling $^{87}\text{Sr}/^{86}\text{Sr}$ in groundwaters along contrasting flowpaths. The glacial outwash comprising the aquifer is derived from Precambrian lithologic sources, providing the potential for an exceptional range of $^{87}\text{Sr}/^{86}\text{Sr}$ among minerals. On the other hand, the generally uniform mineralogic distribution characteristic of outwash deposition, as well as the short weathering history (~10 Ka) of the glacial outwash argue against the potential for large-scale isotopic variability of weathering-derived Sr. Because values of $^{87}\text{Sr}/^{86}\text{Sr}$ having a wide range of from 0.708–0.728 have been measured in waters from the Trout Lake area (Krabbenhoft et al., 1992; Walker et al., 1992; Bullen et al., 1993), understanding the kinetics of mineral-water interaction along contrasting groundwater flowpaths is essential.

2. SITE DESCRIPTION AND PREVIOUS WORK

Our work extends that of Kenoyer and Bowser (1992a,b) who established a piezometer network and studied groundwater chemical evolution across an isthmus that separates two lakes (Crystal and Big Muskellunge) near the top of the watershed. The general geologic framework of the area has been described by Kenoyer and Bowser (1992a), and the pertinent information from that study is summarized here. The aquifer consists of approximately 50 m of sandy glacial outwash which overlies Precambrian bedrock. The glacial sediments comprise the Copper Falls Formation and were eroded from a variety of Precambrian rocks from areas to the north and northeast (Attig, 1985). These rocks include gneiss, amphibolite, schists, granites, monzonites, mafic metavolcanics, and quartzose and feldspathic sandstones (Allen and Barret, 1915).

The isthmus that separates Crystal and Big Muskellunge Lakes is dominated by sand-sized material (85–95%), with minor amounts of clay and silt. Two apparently extensive silt layers that influence the hydrology were identified by Kenoyer and Bowser (1992a) from drilling. It should be noted that the isthmus site lies within a state park and adjacent to a public beach, and thus considerable surface packing due to features such as remnant road beds and camp sites may locally affect the ability of meteoric waters to infiltrate to the water table. Road access is far more limited elsewhere in the watershed.

According to x-ray diffraction analyses reported by Kenoyer and Bowser (1992a), minerals in the sand-sized fraction occur in the following abundances: quartz (50–75%), calcic plagioclase (9–15%), sodic plagioclase (9–15%), K-feldspar (2–10%), biotite (1–2%), opaque minerals (0.5–1.5%), and minor amounts (<1%) of pyroxene, amphibole, epidote, and chlorite. Multi-mineralic igneous and metamorphic rock fragments, referred to herein as MRFs, constitute about 1% of the sand. Clay minerals include smectite (30–40%), illite (30–40%), and chlorite + kaolinite (15–30%). Our observations for this study, using binocular microscope and mineral separation techniques, indicate that quartz may comprise as much as 85%, and hornblende and MRFs >1% of the matrix, with corresponding lesser amounts of the remaining phases. Plagioclase, dark amphibole (hornblende), and green minerals (pyroxene and chlorite?) occur mainly as discrete grains, whereas K-feldspar and biotite dominate the MRFs and may only rarely occur as discrete grains. Carbonate minerals have not been identified in any sample collected from the aquifer, a fact consistent with the low values of $\delta^{13}\text{C}$ (<–16‰) observed in groundwaters from throughout the watershed (Krabbenhoft et al., 1992).

Within the context of this mineralogic assemblage, Kenoyer and Bowser (1992a,b) modeled the chemical evolution of groundwater along the flowpath taken by Crystal Lake water through the isthmus. The location of their modeled flowpath was constrained by measurements of piezometric potential and hydraulic conductivity distribution, as well as by chemical analyses of groundwaters that delineated a plume of relatively low ionic-strength water. Their model for chemical evolution called for dissolution of fixed proportions of An_{41} plagioclase and minor diopside and biotite,

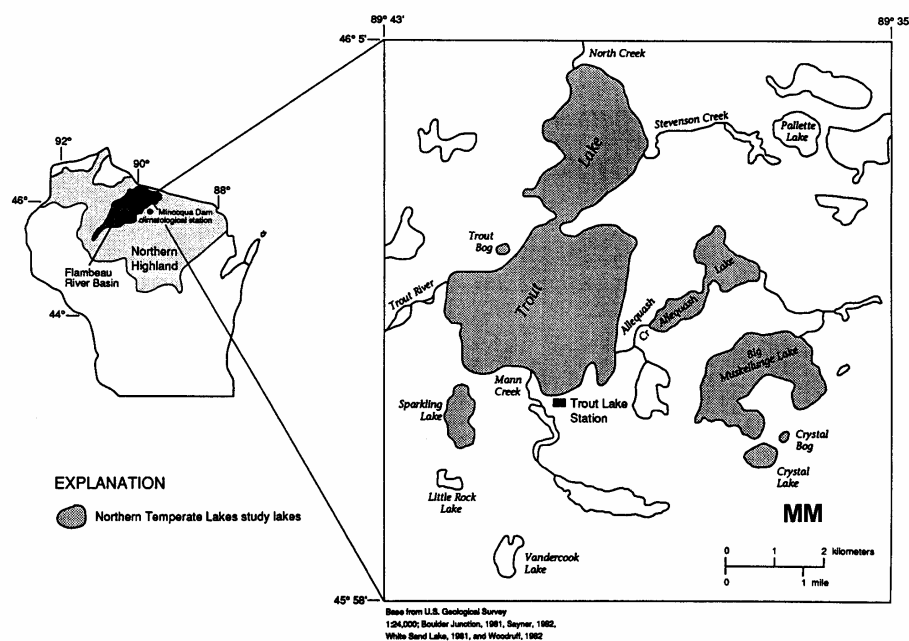


FIG. 1. Crystal Lake is near the head of the watershed; Muskellunge Mountain ("MM" on map), the local topographic high, lies approximately 1.5 km to the southeast of the lake. Groundwater flow lines are generally directed toward Trout Lake at the base of the watershed. The narrow isthmus separating Crystal and Big Muskellunge Lakes is the location of the intensively-sampled aquifer recharge flowpath discussed in this paper. Modified from Elder et al. (1992).

coupled with precipitation of clay (kaolinite, smectite, and/or a metastable gibbsite-kaolinite hybrid). Here we show that the relative contributions from dissolving minerals must change along the lake-water recharge flowpath in order to accurately account for the observed chemical evolution.

3. ANALYTICAL TECHNIQUES

Water samples (groundwater, lake water, precipitation) were filtered through 0.45 μm cellulose nitrate sheets and acidified to pH = 2 with high-purity HNO_3 in the field and stored in sealed polyethylene bottles. Calcium, magnesium, strontium, sodium, potassium, iron, aluminum, and silicon concentrations were measured on a Jarrel Ash® inductively-coupled plasma atomic emission spectrophotometer, using mixed-solute solutions as standards and quality-check replicates. Precision for Na and K is approximately 5%, for Sr is approximately 10% and for all other elements is better than 1%. For chromatographic separation, the water samples were loaded directly onto columns packed with Bio-Rad® AG50X8 cation exchange resin (H^+ -form). Strontium was separated from other cations using HCl as the eluent.

Plagioclase, hornblende, and an aggregate of MRFs were separated from a large composite sample collected from the upper five feet of sand at a site near the middle of the isthmus. The minerals were separated using a combination of heavy liquid, Franz® magnetic separation, selective dye, and manual handpicking techniques. The

separates were totally digested in sealed Teflon® vessels using Teflon®-distilled HF and HNO_3 , and quartz-distilled HCl. Prior to digestion, the plagioclase separate was leached in 8 M HNO_3 and 5% HF to remove labile Sr. An isotopically-enriched Sr-spike solution was added to a small aliquot of each mineral digest for analysis of Sr concentration by isotope dilution. Strontium in the spiked and unspiked mineral fractions was separated from other ions using Bio-Rad® AG50X8 cation exchange resin (H^+ -form) with HCl as the eluent. In all cases, the purified Sr was converted to nitrate form, taken up in 30 μL of 0.15 M H_3PO_4 and loaded onto a single Ta ribbon for mass spectrometric measurement. The approximate total analytical blanks are 4 ng for the mineral separation/digest procedure and 2 ng for the water collection/analysis procedure, both of which are negligible (<0.1%) for these samples.

The isotopic composition of Sr in spiked samples was measured on a Finnigan MAT® 261 multi-collector mass spectrometer, using a static collection mode. Reported Sr concentrations are precise to 1% or better. The isotopic composition of Sr in unspiked samples was measured on the same instrument using a double-collection dynamic mode. All reported values of $^{87}\text{Sr}/^{86}\text{Sr}$ have been corrected for natural and analytical stable isotope fractionation to $^{86}\text{Sr}/^{88}\text{Sr} = 8.37521$, and are precise to 0.00002 or better at the 95% confidence level (2 SDM). This mass spectrometer typically reports a value of 0.71024 for the NBS987 Sr metal standard. Strontium isotope compositions are given both in decimal form and as $\delta^{87}\text{Sr}$, the permil deviation of the sample from the NBS987 standard. Oxygen isotope compositions of lake and lake-bed water samples are reported

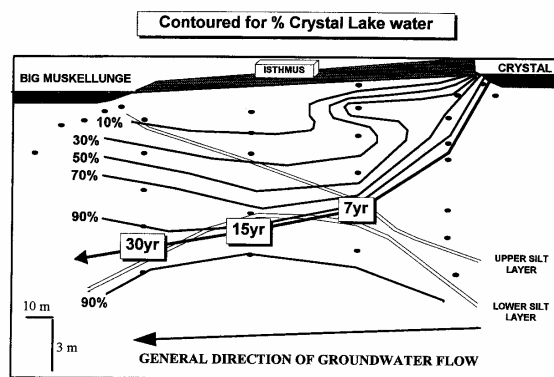


FIG. 2. Groundwater beneath the isthmus is a mixture of Crystal Lake water (evaporated) and precipitation (unevaporated) that infiltrates the isthmus surface. Using a simple linear relation, the proportion of Crystal Lake water in a sample (piezometer points shown as dots) can be calculated using water isotope compositions (i.e., $\delta^{18}\text{O}$ and $\delta^2\text{H}$). The vertical well nest nearest to Crystal Lake is "nest 1" in Table 2; the vertical well nest nearest to Big Muskellunge Lake is "nest 4." The near-isthmus lake-bed wells listed in Table 2 are shown beneath Crystal and Big Muskellunge Lakes. The vector emanating from Crystal Lake delineates the flowpath of groundwater recharge constrained by water isotopes and hydrologic measurements; numbers in boxes are estimated groundwater ages in years based on modeling of tritium concentrations (modified from Krabbenhoft et al., 1996).

as $\delta^{18}\text{O}$, the permil deviation of the sample from V-SMOW, and are precise to 0.1‰.

4. SAMPLING STRATEGY

For this study, groundwater samples were collected from an extensive piezometer network at the isthmus. The vertical and along-gradient distribution of the piezometers is shown in Fig. 2; a map showing their aerial distribution is given in Kenoyer and Bowser (1992a). The chemical and strontium isotope compositions of the groundwater samples are listed in Table 1. Data for two samplings (September, 1992 and June, 1993) along the predominant flowpath of Crystal Lake water through the isthmus as constrained by water isotopes and hydrologic measurements (Krabbenhoft et al., 1996) are given to demonstrate the temporal consistency of groundwater compositions. Except for one deep well (nest 3, K77), there is little temporal change in chemical or strontium isotope compositions.

To assess the chemical and isotopic variability of lake-bed waters, groundwater samples from the beds of Crystal and Big Muskellunge Lakes were collected from newly installed piezometers. At Crystal Lake, porewater from the littoral zone and a deeper groundwater sample were collected. At Big Muskellunge Lake, a five piezometer transect extending outward from the isthmus at a groundwater recharge zone, and a three piezometer transect extending outward from the northeast shoreline at a groundwater discharge zone were sampled. In addition, water samples were collected from five lakes (including Crystal and Big Muskellunge Lakes) that span the hydrologic gradient of the watershed; their locations are shown in Fig. 1. The value of $\delta^{87}\text{Sr}$ for Crystal Lake is the average of five samples (range: -0.12 to $+0.38$), and that for Big Muskellunge Lake is the average of three samples (range: $+6.30$ to $+7.70$) collected at different times of the year. The values for the other lakes represent a single sampling during October, 1991. The extent of stratification of $\delta^{87}\text{Sr}$ in the lakes prior to overturn is not known. Calcium and strontium concentrations, as well as strontium- and oxygen-isotopic data for these samples are listed in Table 2.

To estimate the input of atmospheric Sr to the watershed, strontium isotopes and concentrations were determined in ten samples of rain collected at different times of the year from within the water-

shed, and in a snow sample collected from the isthmus (Table 3). The rain values cluster around $\delta^{87}\text{Sr} \sim 0$, with a range of -2.7 to $+3.1$, and contain between 0.6 and 1.1 $\mu\text{g/L}$ Sr. The snow sample is less radiogenic at $\delta^{87}\text{Sr} \sim -3.4$, and contains 0.5 $\mu\text{g/L}$ Sr. The source of the less radiogenic Sr in the snow is as yet enigmatic, but could be derived by leaching of canopy litter in the accumulating snow pack, or alternatively could represent variability of $\delta^{87}\text{Sr}$ in precipitation from different storm tracks.

Strontium isotope and Ca- and Sr-concentration data for plagioclase, hornblende, and an aggregate of approximately 30 MRFs separated from the aquifer sand are given in Table 4. Of the Sr-bearing minerals present in the sand, only plagioclase and hornblende could be effectively separated as discrete phases in sufficient amounts for analysis. K-feldspar and mica exist as discrete grains (although in minor abundance in our processed sample) but are likewise important components of the MRFs, and thus the rock fragment separate listed in Table 4 contains a large component of these two typically radiogenic phases. A critical observation is that the plagioclase separate has lesser $\delta^{87}\text{Sr}$ (-4.0) and the MRF separate has greater $\delta^{87}\text{Sr}$ ($+18.7$) than most waters yet sampled from the watershed. Moreover, $\delta^{87}\text{Sr}$ of the hornblende separate ($+0.8$) and that of the plagioclase separate bracket all but one of the values observed in groundwaters at the isthmus (Table 1).

5. DISCUSSION

5.1. Strontium Isotopic and Chemical Evolution of Groundwater at the Isthmus

Groundwater at the isthmus is derived by mixing of two water sources: greatly evaporated and thus ^{18}O - and ^2H -enriched Crystal Lake water that emanates from the littoral zone of the lake, and precipitation that infiltrates the isthmus surface. The differences in water isotope compositions of these two water sources provide the basis to contour groundwater with respect to proportion of Crystal Lake water (Krabbenhoft et al., 1996). As shown in Fig. 2, the propor-

TABLE 1. Chemical and strontium isotope data for isthmus groundwaters. Concentrations are in mg/L. Data are for the September, 1992 sampling except where labeled (6/93) which denotes samples collected during June, 1993. Samples are arranged from shallow to deep within individual nests.

sample	Ca	Mg	Sr	Na	K	Fe	Al	Si	$^{87}\text{Sr}/^{86}\text{Sr}$	$\delta^{87}\text{Sr}$
nest 1:										
k1 (shallow)	4.12	0.92	0.017	1.98	0.51	3.00	0.01	0.87	0.71078	+0.76
k85	2.15	0.52	0.012	0.86	0.59	0.00	0.03	0.79	0.71024	0.00
k86	1.73	0.30	0.009	0.64	0.62	0.41	0.00	1.00	0.71018	-0.08
k86 (6/93)	1.96	0.33	0.009	0.57	0.53	0.47	0.04	0.92	0.71018	-0.08
k87	1.70	0.26	0.011	0.61	0.55	0.51	0.00	0.92	0.71008	-0.23
k87 (6/93)	1.89	0.37	0.011	0.59	0.52	0.69	0.23	1.25	0.71018	-0.08
k88	1.79	0.38	0.006	0.90	0.52	0.68	0.00	1.78	0.70949	-1.06
k89	2.81	0.48	0.018	0.95	0.67	0.12	0.00	2.90	0.70832	-2.70
k2 (deep)	5.37	1.97	0.017	1.66	0.59	0.03	0.01	5.08	0.70798	-3.18
nest 2:										
k66 (shallow)	9.42	1.61	0.068	1.53	2.61	26.94	0.02	3.68	0.70953	-1.00
k67	2.28	0.69	0.019	1.25	0.58	2.56	0.00	4.68	0.70812	-2.98
k68	4.26	0.99	0.027	1.35	0.74	0.00	0.00	4.26	0.70814	-2.96
k69	3.55	0.85	0.023	1.39	0.77	0.00	0.00	4.22	0.70815	-2.94
k70	2.62	0.70	0.017	1.20	0.54	0.21	0.00	4.08	0.70778	-3.46
k70 (6/93)	2.70	0.70	0.015	1.13	0.50	0.19	0.02	3.85	0.70786	-3.35
k71 (deep)	6.41	2.69	0.018	1.58	0.61	0.02	0.00	6.20	0.70741	-3.98
nest 3:										
k73 (shallow)	4.30	1.36	0.029	1.42	1.64	3.78	0.03	4.71	0.71213	+2.66
k74	3.56	1.36	nd	nd	nd	nd	nd	6.71	0.71026	+0.03
k75	2.39	0.65	0.018	1.49	0.58	4.75	0.00	5.17	0.70805	-3.08
k76	3.58	1.56	0.019	1.79	0.79	4.15	0.05	6.82	0.70771	-3.56
k76 (6/93)	3.51	1.50	0.018	1.89	0.64	5.91	0.01	7.23	0.70794	-3.24
k77 (deep)	3.09	1.03	0.006	0.40	1.60	0.58	0.11	0.34	0.71130	+1.49
k77 (6/93)	8.92	3.88	0.057	1.87	1.32	2.72	2.79	12.53	0.70827	-2.77
nest 4:										
k6 (shallow)	3.82	1.50	0.024	1.62	1.04	10.41	0.03	6.53	0.70969	-0.77
k80	3.72	1.93	0.012	2.56	0.56	6.15	0.02	7.55	0.70871	-2.15
k81	5.13	2.32	0.016	2.04	0.58	4.76	0.00	7.35	0.70782	-3.41
k82	7.05	3.25	0.018	1.77	0.58	1.94	0.01	11.03	0.70756	-3.77
k82 (6/93)	7.01	3.16	0.018	1.68	0.56	2.22	0.00	9.09	0.70756	-3.77
k5 (deep)	7.43	3.15	0.017	1.59	0.59	0.49	0.01	8.85	0.70825	-2.80
k5 (6/93)	7.94	3.23	0.017	1.43	0.63	0.42	0.00	8.41	0.70821	-2.86

tion of Crystal Lake water in groundwater generally increases with depth. The trajectory of the predominant flow-path (i.e., center of mass) of Crystal Lake water as it recharges the aquifer is initially steep, but flattens considerably upon intersecting the silt layers.

The majority of water samples collected from piezometers at the isthmus have less radiogenic Sr than that observed in

both Crystal Lake water and average precipitation ($\delta^{87}\text{Sr} \sim 0$), and span a range of $\delta^{87}\text{Sr}$ of from -4.0 to $+2.7$ (Table 1). The two samples having $\delta^{87}\text{Sr} > 0$ are both the shallowest wells in their nests, and thus contain the greatest proportion of infiltrating precipitation. The strontium isotope data for the groundwater and lake bed wells are used to generate a strontium isotope contour plot (Fig. 3). The posi-

TABLE 2. Chemical and isotopic data for lake and lake bed wells. Concentrations are in mg/L.

sample	Ca	Sr	$^{87}\text{Sr}/^{86}\text{Sr}$	$\delta^{87}\text{Sr}$	$\delta^{18}\text{O}$
Crystal Lake	1.13	0.004	0.71041	+0.24	-3.2
porewater	1.08	0.008	0.71166	+2.00	-3.4
lake bed well 1	1.34	0.007	0.71059	+0.49	-3.9
Big Muskellunge Lake					
lake bed transect near isthmus:	6.70	0.013	0.71530	+7.12	-4.9
well 1 (nearest shore)	4.85	0.020	0.70776	-3.50	-4.9
well 2	9.09	0.020	0.70875	-2.10	-5.2
well 3	10.42	0.022	0.70847	-2.50	-5.5
well 4	9.98	0.037	0.70821	-2.90	-5.2
well 5 (farthest from shore)	11.75	0.028	0.70860	-2.30	-5.8
lake bed transect at NE shoreline:					
gw discharge well 1 (near shore)	24.00	0.033	0.72686	+23.4	-11.6
gw discharge well 2	20.54	0.035	0.71900	+12.33	-11.3
gw discharge well 3	15.49	0.030	0.71647	+8.77	-11.5
Little Rock Lake					
Sparkling Lake	1.20	0.005	0.71093	+0.94	-4.2
Trout Lake	9.80	0.017	0.71591	+7.95	-5.8
	12.50	0.023	0.71976	+13.38	-9.0

TABLE 3. Strontium isotope and concentration data for rain collected from Trout Lake Station and from near Allequash Creek to the north of Big Muskellunge Lake, and for snow collected from the isthmus study site. Concentrations are in mg/L.

date	location	$^{87}\text{Sr}/^{86}\text{Sr}$	$\delta^{87}\text{Sr}$	Sr
7/2/92	Trout Lake Station	0.71020	-0.06	0.63
6/21/93	Allequash Creek, Lower Site	0.71244	+3.10	0.72
6/21/93	Allequash Creek, Middle Site	0.71059	+0.49	0.81
6/21/93	Allequash Creek, Upper Site	0.71078	+0.76	0.75
8/6/93	Allequash Creek, Lower Site	0.71040	+0.23	0.84
8/6/93	Allequash Creek, Middle Site	0.71000	-0.34	0.78
8/6/93	Allequash Creek, Upper Site	0.71065	+0.58	0.79
9/15/93	Allequash Creek, Lower Site	0.70833	-2.69	1.06
9/15/93	Allequash Creek, Middle Site	0.70856	-2.37	0.92
9/15/93	Allequash Creek, Upper Site	0.70980	-0.62	0.88
2/4/93	Isthmus at Crystal Lake (snow)	0.70781	-3.42	0.57

tions of the silt layers and the vector describing the center of mass of the groundwater-recharge plume emanating from Crystal Lake are included for reference (Krabbenhoft et al., 1996). The most salient features of this diagram are that $\delta^{87}\text{Sr}$ becomes progressively more negative along the predominant lakewater flowpath, and that the contours generally mirror the orientation of the silt layers. Furthermore, although $\delta^{87}\text{Sr}$ generally decreases with depth, that trend reverses itself in the deepest piezometers of the two nests nearest to Big Muskellunge Lake. Overall, $\delta^{87}\text{Sr}$ contours are tightest above the upper silt layer.

There are three additional important observations to be made from Fig. 3. First, assuming that Big Muskellunge Lake is well-mixed in terms of Sr and thus isotopically homogeneous, Sr in the lake is far more radiogenic ($\delta^{87}\text{Sr} = +7.1$; Table 2) than any groundwater sampled from the isthmus, and there is more change in $\delta^{87}\text{Sr}$ across the sediment-water interface of Big Muskellunge Lake than at any location across the isthmus. This is true even though the waters sampled from the lake bed piezometers along the transect extending outward from the isthmus clearly contain predominantly lake water, based on the water isotopes (Table 2). Second, based on the observation that samples from the uppermost piezometers in each nest have the greatest $\delta^{87}\text{Sr}$ (as high as +2.7) and significantly higher Sr concentrations than precipitation, waters that recharge the water table through the isthmus surface are probably more radiogenic than the precipitation endmember ($\delta^{87}\text{Sr} \sim 0$; Table 3), perhaps due to reactions with minerals in the thin unsaturated zone. Third, the strontium isotope contours bulge at piezometer nest 2, which lies directly beneath the site of an old road bed. The remnant roadbed may greatly retard the infiltration of water through the thin unsaturated zone. This is consistent with the observation, based on the water isotopes (Fig. 2), that the water sampled by the uppermost piezometer in this nest is similar to precipitation, whereas the water sampled by the immediately underlying piezometer contains a significant component of Crystal Lake water (Krabbenhoft et al., 1996). Alternatively, the degrading roadbed materials may provide a localized source of relatively unradiogenic Sr.

Concentrations of Si, Ca, Mg, Sr, Na, and Fe are generally least in the piezometer nest nearest to Crystal Lake and increase down gradient. Due to the diagonal trajectory of the predomi-

nant flowpath of Crystal Lake water across the isthmus, contour plots provide the most straightforward approach to considering cross-isthmus chemical variability. Contour plots of dissolved Si and Ca concentrations, both distinctive measures of chemical evolution at the isthmus, are shown in Fig. 4a and 4b. The contour patterns for Mg, Na, and Sr concentrations (not shown) generally mimic that of Ca, although as discussed below significant downgradient deviations occur for Na and Sr. Potassium concentrations show no systematic variability across the isthmus, and only one of the isthmus groundwater samples contains significant Al.

Overall, the contour pattern for dissolved Si is uncomplicated and is controlled in part by the position of the silt layers. The contour pattern for dissolved Ca is more complex, particularly in the upper portion of the aquifer. Regardless, the important observation is that Si and Ca concentrations persistently increase along the lake-water recharge flowpath. The occurrence of low Ca concentrations at intermediate depths in each piezometer nest in part led Kenoyer and Bowser (1992a) to postulate a shallower cross-isthmus flowpath for groundwater recharge as a low ionic-strength plume out of Crystal Lake. In fact there is only a weak chemical plume structure along the predominant flowpath defined by water isotopes, prior to its intersection with the lower silt layer.

In Fig. 5a, normalized concentrations of Si, Ca, Mg, Sr, Na, and Fe at sampling sites along the lake-water recharge flowpath are plotted against groundwater age. The concentrations are normalized to the maximum values attained along the flowpath in order to mask absolute concentration differences among these elements. The estimates of groundwater age are based on modeling of measured tritium concentrations (Krabbenhoft et al., 1996). Silicon, calcium, magnesium, and particularly Sr and Na concentrations progressively increase along this flowpath for approximately the first 15 years of chemical evolution; Fe increases over that time period in a more irregular manner. Beyond that point, which corresponds to interception of the silt layers, Na, Sr, and Fe concentrations level off or decrease (substantially in the case of Fe), and Si concentrations rise less rapidly as Ca and Mg concentrations continue to increase. The tendency of Sr to remain constant while Ca increases is particularly intriguing and suggests an along-flowpath change in relative contributions from dissolving mineral phases.

In Fig. 5b, the net molar addition rates (i.e., μmol of solute per liter added per year) of Si, Ca, Mg, and Na for three time periods along the lake-water recharge flowpath are plotted against the average groundwater age for each period. In general, the net rates of Ca and Mg addition remain relatively constant along the flowpath. In contrast, the net rates of Si and Na addition progressively decrease along the flowpath. In the young-

TABLE 4. Chemical and strontium isotope data for mineral separates. Concentrations are in parts per million.

phase	$^{87}\text{Sr}/^{86}\text{Sr}$	$\delta^{87}\text{Sr}$	Ca	Sr
plagioclase	0.70741	-4.00	59071	610
hornblende	0.71082	0.82	80682	78
multi-mineralic rock fragments	0.72350	18.67	4210	385

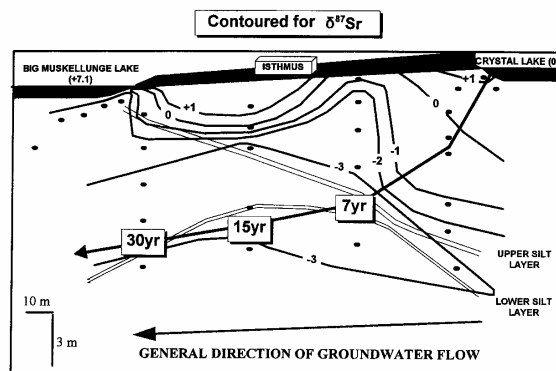


FIG. 3. Contour plot of strontium isotope composition of groundwaters across the isthmus. In general the distribution of the contours parallels that of two extensive silt layers. $\delta^{87}\text{Sr}$ progressively decreases along the dominant flowpath of groundwater recharge emanating from Crystal Lake.

gest time period, the greater molar addition rates of (Ca + Na) relative to that of Mg and of Si relative to that of (Ca + Na + Mg), as well as the substantial addition rate of Sr (not shown) are all consistent with dissolution of plagioclase feldspar. In the oldest time period, the greater molar addition rate of (Ca + Mg) relative to that of Si, and the lesser Na (and Sr) addition, are consistent with dissolution of a Na- and Sr-poor ferromagnesian phase such as hornblende or augite and a significantly reduced role for plagioclase dissolution. The absence of dissolved Al requires continuous along-flowpath formation of clays which regulate K concentrations and may incorporate some Na and Sr. The strong decrease in Fe concentrations in the oldest time period (Fig. 5a) may indicate the precipitation of a phase such as an Fe-oxyhydroxide that likewise may incorporate or sorb other cations.

In order to test whether the apparent change in relative contributions from these minerals can be attributed to their theoretical thermodynamic behavior, the computer code SOLMINEQ.88 (Kharaka et al., 1988) was used to calculate ideal mineral saturation indices for groundwaters along the lakewater recharge flowpath. The calculated values are listed in Table 5, and the ranges defined by the endmembers of each mineral phase are plotted in Fig. 6 as a function of groundwater age. Saturation indices of plagioclase, pyroxene, biotite, and amphibole are most negative for the youngest groundwaters, and progressively increase but remain negative with increasing groundwater age. Although the values for the different minerals are not strictly comparable, saturation indices of these minerals increase by similar relative amounts over the 30 year time span of the flowpath, suggesting that plagioclase is not becoming preferentially less soluble due to changes in water chemistry alone.

5.2. Strontium Isotopic Composition of Groundwater Derived From Upland Areas

Krabbenhoft et al. (1994) used $\delta^{18}\text{O}$, δD , and the chemistry of several lakes from the region to show that the lakes

define a mixing trend in $\delta^{18}\text{O} - \delta\text{D}$ space between the average composition of local precipitation ($\delta^{18}\text{O} = -11.3$) and an enriched composition ($\delta^{18}\text{O} \sim -3$) resulting from evaporation of meteoric water in lakes. Further, $\delta^{18}\text{O}$ and δD of lake water become increasingly similar to the average value of precipitation with increasing groundwater contribution to the lakes (i.e., increasing conductivity). Therefore, although isotopically-enriched groundwaters derived from upgradient lakes may contribute to discharge at downgradient lakes, most of that discharge must be supplied along flowpaths originating in the inter-lake uplands to avoid isotopic enrichment. For example, the samples of groundwater discharge to Big Muskellunge Lake (Table 2) are clearly not evaporated. The restricted values of $\delta^{18}\text{O}$ in these samples (-11.6 to -11.3) are essentially identical to the groundwater endmember postulated by Krabbenhoft et al. (1990) for lakes in this region. The logical source of these groundwater discharge samples is meteoric water that infiltrates the adjacent uplands and recharges the local water table.

Compared to groundwaters at the isthmus, the samples of groundwater discharging to Big Muskellunge Lake contain substantially more radiogenic Sr ($\delta^{87}\text{Sr} = +8$ to $+23$; Table 2). A plausible explanation for this difference is that flowpaths originating in upland areas pass through a thicker unsaturated zone than is present at the isthmus between Crystal and Big Muskellunge Lakes, providing a different physico-chemical environment for the solution of Sr and other cations. At the aquifer discharge transect, $\delta^{87}\text{Sr}$ and Ca concentrations decrease away from the shoreline whereas Sr concentrations are constant. The sample collected nearest to shore and having the greatest $\delta^{87}\text{Sr}$ and Ca concentration reflects discharge of the shallowest groundwater to the lake, and thus should have the greatest relative contribution from the unsaturated zone of the adjacent upland. The correlation of $\delta^{87}\text{Sr}$ with Ca concentration and the lack of correlation with Sr concentration in the groundwater discharge samples suggests that residence time in the unsaturated zone leads to

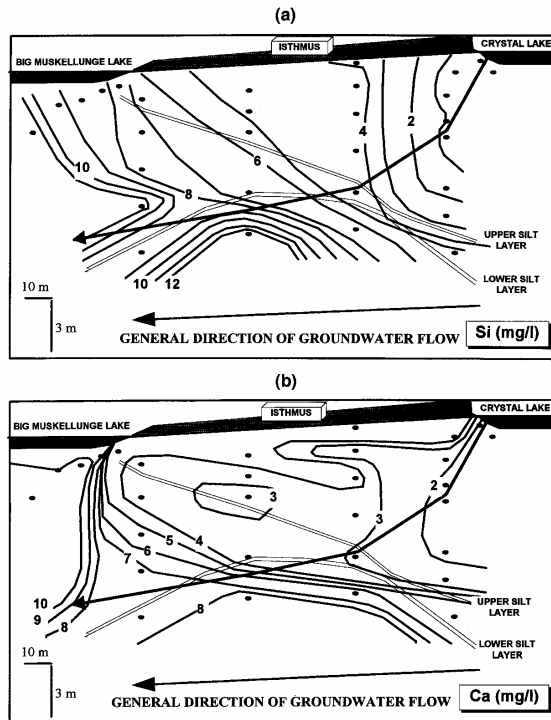


FIG. 4. (a) Contour plot of dissolved Si in isthmus groundwaters. The generally-smooth pattern of increasing values across the isthmus demonstrates that Si provides a convenient measure of chemical evolution. (b) Contour plot of dissolved Ca in isthmus groundwaters. The pattern is more complex than that for Si, revealing an apparent low ionic-strength plume that lies well above the actual predominant flowpath of groundwater recharge emanating from Crystal Lake.

elevated Ca concentrations, Ca/Sr ratios, and $\delta^{87}\text{Sr}$ in the infiltrating meteoric waters. Interestingly the highly-radiogenic Sr is probably derived from a phase such as K-feldspar or biotite, neither of which contain significant Ca.

$\delta^{87}\text{Sr}$ of the lakes spans a broad range (0 to +13.5), and increases as Ca and Sr concentrations increase and $\delta^{18}\text{O}$ decreases (Table 2). On a plot of $\delta^{18}\text{O}$ vs. $\delta^{87}\text{Sr}$ (Fig. 7), the lake data define a distribution that is consistent with mixing of two water types: evaporated meteoric water having relatively low Sr concentration and low $\delta^{87}\text{Sr}$, and groundwater having relatively high Sr concentration and high $\delta^{87}\text{Sr}$. On this type of diagram, various mixtures of two endmembers define a hyperbola. The curve drawn through the data in Fig. 7 is based on the following end conditions: $\delta^{87}\text{Sr} = -1$, an average value for the snow and precipitation samples, for the evaporated meteoric component; and $\delta^{18}\text{O} = -11.3$, average local precipitation determined by Krabbenhoft et al. (1990), for the groundwater component. The curvature of

the hyperbola is determined by the approximately eightfold difference in Sr concentration between Crystal Lake water, which is dominated by evaporated meteoric water, and the samples of groundwater discharge to Big Muskellunge Lake. $\delta^{87}\text{Sr}$ of the groundwater component predicted by this hyperbola is approximately +15. Taken together, the samples of groundwater discharge to Big Muskellunge Lake effectively bracket this calculated groundwater component.

5.3. Experimental Constraints on Strontium Isotope Evolution

The decrease in $\delta^{87}\text{Sr}$ and the accompanying change in water chemistry along the groundwater recharge flowpath emanating from Crystal Lake suggests that the waters obtain their Sr predominantly from plagioclase and hornblende. In contrast, along the recharge pathways originating in upland areas, phases such as K-feldspar and biotite that contain far

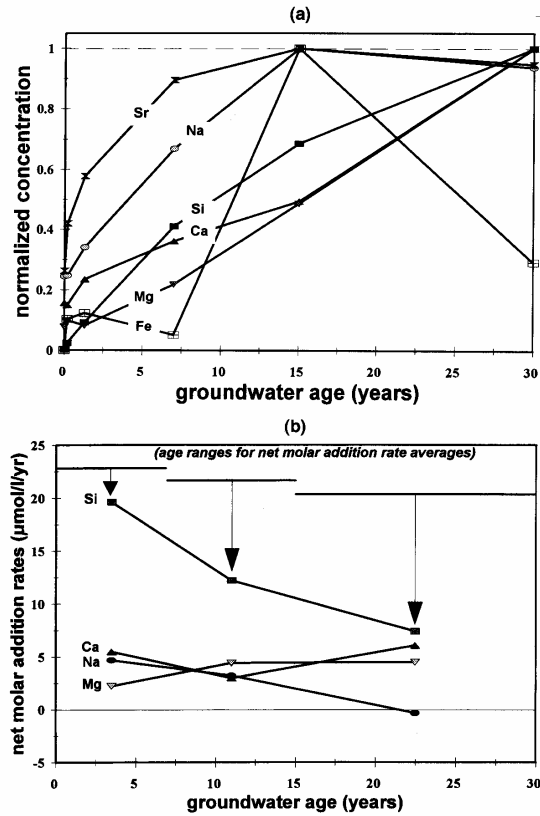


FIG. 5. (a) Variation in water chemistry at sampling points along the predominant flowpath of groundwater recharge emanating from Crystal Lake (September, 1992 data from Table 1). Sample points and ages used: Crystal Lake (0 years); Crystal Lake porewater (0.2 years); K87 (1.25 years); K70 (7 years); K76 (15 years); average of K82 and K5 (30 years). (b) Net molar addition rates of selected elements along the predominant flowpath of groundwater recharge emanating from Crystal Lake. Average rates are shown for three time periods. The ratios of alkali and alkali-earth cations to silica are consistent with dissolution of plagioclase in the young waters, and of a calcic ferromagnesian silicate mineral(s) in the older waters.

more radiogenic Sr apparently control the strontium isotope composition. An important difference between these two pathways is that water is continuously moving along the saturated lake-water recharge flowpath, whereas episodic recharge in the uplands may be periodically immobilized in the unsaturated zone. In order to test whether the observed differences in the isotopic composition of dissolved Sr might result from differences in water mobility, an experiment was designed using a column packed with sand from the isthmus and deionized (DI) water as the eluent.

To begin the experiment, a slurry of DI water and 500g of the sand sample used to obtain mineral separates was

placed in a glass column containing a porous frit at its base. After the initial water had drained, the air space in the column above the sand was filled with DI water and the level was held constant for the first four collection periods during which the water dripped through at a rate of 5 mL/min. The first 100 mL and the following three 300 mL of DI water passed through the column were collected for analysis. Subsequently, the column was allowed to drain and sit for a period of about 12 hours, and then was refilled with DI water and maintained at constant level for five additional collections at a similar drip rate. The first 100 mL and the following four 500 mL of DI water passed through the col-

TABLE 5. Saturation indices along groundwater recharge flowpath from Crystal Lake.

	Crystal Lake	porewater	k66	k70	k76	k5
age (years)	0	0	1.3	7	15	30
mineral:						
Albite	-11.1	-8.8	-6.4	-4.1	-2.8	-2.5
Anorthite	-10.0	-9.0	-7.0	-5.2	-4.2	-3.2
K-feldspar	-6.2	-3.8	-1.7	+0.3	+1.2	+1.9
Enstatite	-9.6	-8.4	-8.8	-7.3	-6.0	-4.3
Diopside	-15.4	-15.1	-13.8	-10.9	-8.6	-6.0
Pargasite	-57.7	-57.1	-52.2	-43.2	-35.9	-25.9
Tremolite	-52.8	-50.7	-45.7	-34.9	-26.1	-13.6
Phlogopite	-20.3	-20.0	-18.1	-13.4	-9.4	-3.7
Annite	-17.5	-12.3	-10.6	-8.1	-0.6	+0.7
Illite	-6.0	-3.3	-0.5	+1.9	+2.9	+3.1
Smectite	-4.9	-1.8	+1.3	+3.6	+4.4	+3.8

umn were collected for analysis. In addition, for comparative purposes several grams of the sand were allowed to sit for 12 hours in a beaker containing warm ($\sim 30^\circ\text{C}$) 0.01 N HCl, and the solution was decanted for analysis. The experimental data are given in Table 6, and plotted in Fig. 8.

Nearly the entire range of $\delta^{87}\text{Sr}$ observed in groundwaters from the Trout Lake watershed was observed in waters sampled from the column. $\delta^{87}\text{Sr}$ was greatest in the first aliquot of water passed through the column, and became progressively less positive with successive additions. Following the 12 hour pause, $\delta^{87}\text{Sr}$ returned to a very positive value and then decreased with successive additions of water. The speed with which $\delta^{87}\text{Sr}$ was modified following initiation of fluid movement through the sand is particularly surprising. In contrast, $\delta^{87}\text{Sr}$ obtained in three static leaching experiments using the warm 0.01 N HCl was remarkably constant with values ranging from +10.5 to +11.3.

A simple explanation of the experimental results is suggested by differences in the way that Sr is lost from the various minerals that comprise the sand. The strontium isotope composition of the experimental product waters appears to be controlled by two groups of minerals, those with low $\delta^{87}\text{Sr}$ (predominantly plagioclase and/or hornblende) that

dominate when water moves through the sand matrix (saturated conditions), and those with high $\delta^{87}\text{Sr}$ (predominantly K-feldspar and/or biotite) that dominate when water stagnates within the sand matrix (unsaturated conditions). Strontium loss from plagioclase is accompanied by loss of other cations that either go into solution (i.e., Ca, Na, Si; Fig. 5b) or recombine to form clay minerals (i.e., Al and Si). Hornblende weathering involves the incongruent loss of cations including Al to solution (Zhang et al., 1993), with Al recombining with Si to form clay minerals. In contrast, in young weathering systems Sr can be selectively leached from the lattice of chemically-resistant K-feldspar with little corresponding mass loss of other cations (Bullen et al., 1996). Biotite weathers primarily by conversion to hydrobiotite or vermiculite (Cleaves et al., 1970; Velbel, 1985), and loss of interlayer Sr and other cations occurs to relieve the charge imbalance resulting from oxidation of Fe (White and Yee, 1985).

When waters move continuously through the sand matrix, the clays that form in response to dissolution of aluminosilicate minerals are probably carried in suspension and are unlikely to accumulate on specific reactive phases. Under these conditions, the flux of relatively unradiogenic Sr from

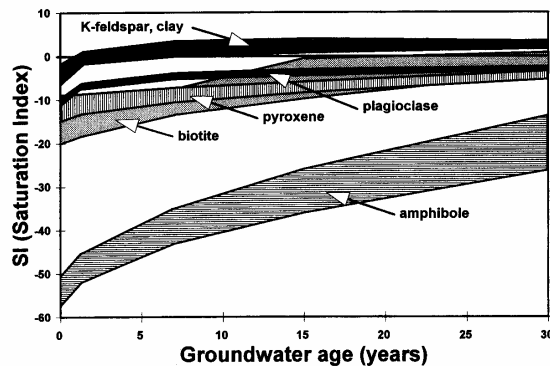


FIG. 6. Saturation indices for groundwaters along the predominant flowpath of recharge emanating from Crystal Lake. Negative values indicate under-saturation, positive values indicate over-saturation with respect to a phase.

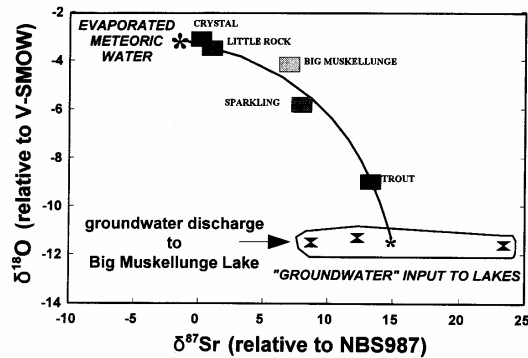


FIG. 7. Hypothetical mixing hyperbola to describe the strontium and oxygen isotopic compositions of lakes in the watershed. The lakes can be described as mixtures of evaporated meteoric water and groundwater that discharges to the lakes; these presumed endmembers are denoted by stars. Three samples of groundwater discharge to Big Muskellunge Lake bracket the modeled value of the groundwater endmember.

plagioclase and hornblende overwhelms that from the other Sr-bearing minerals. In contrast, when waters stagnate or form only thin films and unconnected pore fillings, clay minerals probably precipitate on the surfaces of the minerals that are supplying Al and Si, and thus are more likely to poison the surfaces of plagioclase and hornblende than those of K-feldspar and biotite. This is particularly true for this quartz-rich sand in which grains of plagioclase and hornblende may not typically be in contact with grains of other Sr-bearing minerals. Thus under stagnant conditions, the flux of relatively radiogenic Sr from minerals such as K-feldspar and biotite overwhelms that from hornblende and plagioclase, as well as that from low-Al minerals such as pyroxene and epidote that presumably contain unradiogenic Sr.

5.4. The Transient Role of Plagioclase

Plagioclase feldspar and hornblende are likely to be important reactive phases as groundwater evolves chemically in silicate terrains (Garrels and Mackenzie, 1967; Nesbitt

and Young, 1984; Kenoyer and Bowser, 1992b). Although surface area-dependent dissolution rates for plagioclase observed in the laboratory and in the field are comparable to those for hornblende, mass loss from plagioclase due to weathering generally occurs at a far slower rate than that from hornblende, presumably due to the greater reactive surface area of hornblende grains (White et al., 1996). Thus, one of the more surprising conclusions of the present study is that plagioclase dissolution clearly dominates the first 15 years of chemical evolution along the groundwater flowpath emanating from Crystal Lake, then becomes insignificant relative to hornblende dissolution during the second 15 years of chemical evolution (Fig. 5a,b). Of course, in the absence of core samples from the isthmus we are unable to completely discount the possibility of the sudden disappearance of plagioclase from the aquifer mineral assemblage along the latter part of the flowpath. However, visual examination of sand from numerous locations throughout the watershed reveals that plagioclase is a ubiquitous and relatively abundant mineral phase.

The importance of plagioclase dissolution relative to that of hornblende (or some other calcic ferromagnesian mineral) in the chemical evolution of the groundwaters can be discerned using Ca/Sr ratios, as shown in Fig. 9. Based on the chemical data in Table 4, congruent dissolution of plagioclase and hornblende defines trends on a Ca vs. Sr plot having slopes of approximately 100 and 1000, respectively. All but one of the isthmus groundwater samples collected from above the silt layers lie on or close to a line having a slope (~145) just slightly greater than that defined by plagioclase dissolution. In contrast, most of the samples collected from below the silt layers have greater Ca/Sr ratios, the values being limited by that defined by the data for lakes in the region and the samples of groundwater discharge to Big Muskellunge Lake. This limiting value (~650) is somewhat less than that defined by dissolution of hornblende and probably other calcic ferromagnesian phases. Apparently

TABLE 6. Results of column and static leach experiments.

column experiment:		
volume increment of DI H ₂ O (ml)	⁸⁷ Sr/ ⁸⁶ Sr	δ ⁸⁷ Sr
0-100	0.7220	16.53
100-400	0.7190	12.31
400-700	0.7144	5.83
700-1000	0.7114	1.61
(12 hour pause)		
1000-1100	0.7194	12.87
1100-1600	0.7153	7.10
1600-2100	0.7138	4.98
2100-2600	0.7118	2.17
2600-3100	0.7082	-2.90
static leach experiment:		
beaker	⁸⁷ Sr/ ⁸⁶ Sr	δ ⁸⁷ Sr
beaker 1	0.7177	10.51
beaker 2	0.7180	10.89
beaker 3	0.7182	11.32

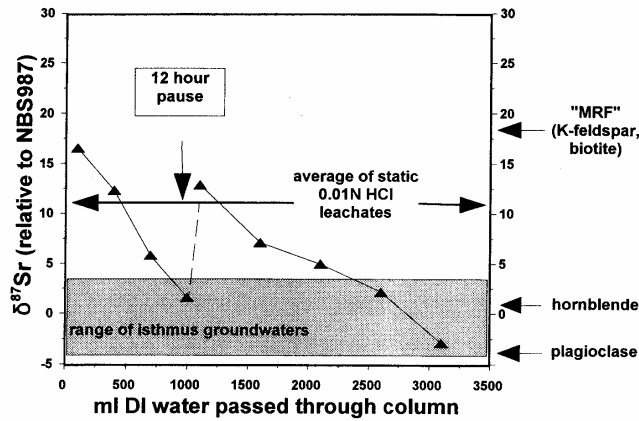


FIG. 8. Results of experiments discussed in the text. The column experiment waters obtain Sr primarily from plagioclase and hornblende under mobile conditions, and from K-feldspar and biotite under stagnant conditions. Three weak-acid leaches of aquifer sand span a narrow range of $\delta^{87}\text{Sr}$ of from +10.5 to +11.3.

plagioclase dissolution is enhanced in the hydrochemical environment that exists above the silt layers at the isthmus.

There are two plausible and probably interrelated explanations for the initially strong but progressively decreasing influence of plagioclase along groundwater flowpaths at the isthmus. First, with progressive chemical evolution the groundwaters closely approach calculated thermodynamic

saturation with plagioclase (Table 5; Fig. 6). Although all waters reported here have negative calculated saturation indices for plagioclase, the more evolved waters are effectively so close to saturation with plagioclase that the dissolution rate may become prohibitively slow. This explanation is consistent with recent experimental evidence which suggests that the dissolution rate of albite in aqueous solutions de-

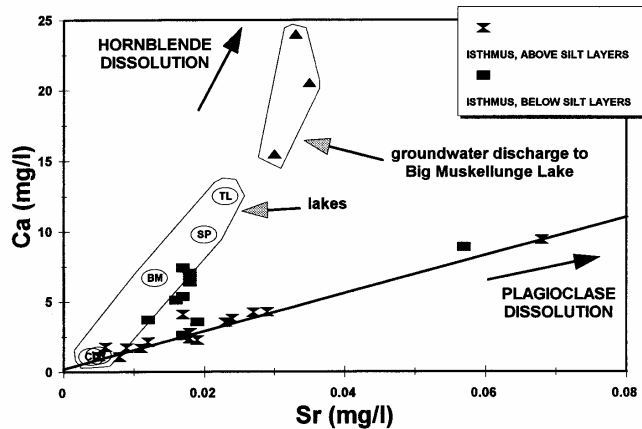


FIG. 9. Groundwater samples collected from above the silt layers at the isthmus form a strong trend on this plot that is similar to the trend resulting from plagioclase dissolution. In contrast, samples collected from below the silt layers trend toward higher Ca/Sr ratios, with values limited by the trend defined by lakes of the region and the samples of groundwater discharge to Big Muskellunge Lake. Symbols for lakes are as follows: CL = Crystal Lake, LR = Little Rock Lake, BM = Big Muskellunge Lake, SP = Sparkling Lake, TL = Trout Lake.

creases abruptly in a sharp stepwise manner at the critical level of undersaturation when etching of dislocation sites on grain surfaces ceases (Burch et al., 1993). Dissolution rates following the step decrease may be more typical of long-term rates observed in field studies of weathering.

Second, following the step decrease in dissolution rate, the surfaces of the plagioclase grains may provide a more stable substrate for Fe-rich precipitates than those of the more reactive ferromagnesian minerals, thus reducing access of weathering solutions to plagioclase grain surfaces. This explanation is consistent with the association of decreased elemental contributions from plagioclase and rapidly decreasing measured Fe concentrations during the second 15 years of chemical evolution along the lake-water recharge flowpath at the isthmus (Fig. 5a). However, because the Fe analyses reported here are probably not representative of true dissolved concentrations, confirmation of this process awaits a more rigorous determination of Fe concentrations using ultrafiltration techniques as well as a study of secondary Fe mineral precipitation in the aquifer.

Our evidence for changing contributions from minerals along the lake-water recharge flowpath calls into question mass balance models that rely on dissolution of minerals in fixed proportions. For example, in their reaction path modeling of groundwater chemical evolution at this site, Kenoyer and Bowser (1992b) invoked dissolution of An_{41} plagioclase, biotite, and augite in a fixed molar ratio of 11:1:1, with concomitant precipitation of a clay phase. These proportions were chosen to satisfy the average increases of Ca, Na, and Mg in the groundwaters during the first three years of evolution along their flowpath. For the remainder of the flowpath, however, the reaction mass balance predicted greater Na and lesser Si in solution compared to observed concentrations, even when precipitation of Na-beidellite and a hypothetical low-Si/Al gibbsite-kaolinite hybrid were invoked. In fact, the mismatch for both Na and Si can be removed simply by reducing the available proportion of plagioclase in the reactant assemblage, thus reducing the amount of Si-bearing clay precipitation that must occur. Clearly, the importance of varying the proportions of both dissolving and precipitating phases must be evaluated for any reaction mass balance. As shown here, consideration of Ca/Sr variations should be useful for determining the relative contributions from plagioclase and calcic ferromagnesian minerals.

5.5. The Natural Variability of the Weathering Signal

Numerous previous investigations referenced earlier have documented that a range of strontium isotope composition can be expected in surface and groundwaters at the watershed scale as a result of both heterogeneities in mineralogic distribution and variations in the contribution of atmospheric components. The additional insight provided by the present study is that strontium isotope composition, and thus contributions from minerals that provide solutes, can likewise be expected to vary in response to both progressive changes in mineral solubilities along flowpaths and differences in fluid mobility along contrasting flowpaths. A simple weak-acid leach of an aquifer material that contains several reactive minerals is an unreliable method for determination of the weathering

contribution. A technique similar to our column experiment may provide a better indication of the range of strontium isotope compositions expected of a given aquifer material.

In the present study, the greater $\delta^{87}\text{Sr}$ of groundwater discharge to Big Muskellunge Lake relative to that in samples along the lakewater recharge flowpath through the isthmus is attributed primarily to enhanced leaching of Sr from relatively unreactive K-feldspar and biotite, coupled with suppressed dissolution of plagioclase during stagnation of infiltrating waters in the unsaturated zone of upland areas. This scenario requires that the surfaces of K-feldspar and biotite grains remain free from the buildup of clay minerals, a condition that may be particularly valid for this quartz-rich sand. Given the same reactive minerals, the range of $\delta^{87}\text{Sr}$ obtained by groundwaters would probably be far less in a quartz-poor matrix, in which the surfaces of K-feldspar and biotite grains would be more susceptible to poisoning by clay mineral aggregates. Regardless, the effect of changing contributions from minerals along a flowpath through such a quartz-poor aquifer material could lead to significant variability of $\delta^{87}\text{Sr}$ in groundwaters, particularly if the plagioclase and calcic ferromagnesian phases are derived from substantially different lithologies.

In addition, redox conditions and their effect on biotite reactivity may play an auxiliary role in promoting the strontium isotopic contrasts observed. White and Yee (1985) demonstrated that selective alkali and alkali-earth cation loss from biotite occurs under oxidizing conditions in order to maintain charge balance in the lattice as Fe^{2+} is converted to Fe^{3+} . The oxidizing conditions of the unsaturated zone should provide a suitable environment for the release of highly-radiogenic Sr from biotite, whereas the reducing conditions along an aquifer recharge flowpath emanating from a lake bottom should inhibit this process. The field observations are consistent with a redox control on the strontium isotopic composition of the groundwaters, but its importance relative to the effects of differential water mobility cannot be determined with the present data.

6. SUMMARY

The traditional approach to understanding the evolution of water chemistry in silicate aquifers has been to assume a quasi steady-state situation in which aluminosilicate minerals that are thermodynamically undersaturated with respect to the water react through complex hydrolysis/carbonation reactions in relatively fixed proportions to provide solutes and form secondary phases. Chemical heterogeneities are typically thought to develop primarily due to factors such as differences in mineral proportions and redox conditions along different flowpaths. This study showcases the power of the combined use of strontium isotopes, water isotopes, and water chemistry to understand how mineral dissolution reactions may change along flowpaths, and differ along contrasting flowpaths.

The most striking conclusion of this study is that such a broad range of $\delta^{87}\text{Sr}$ is produced by weathering. Moreover, the range observed is not due to differences in macro-scale mineral distribution, but rather to the initial environmental conditions along two contrasting groundwater recharge

flowpaths. On one hand, the combined effects of continuous recharge of low ionic-strength water from a lake bed and the reducing character of this environment promote the early dominance of plagioclase dissolution and inheritance of relatively unradiogenic Sr along groundwater recharge flowpaths emanating from lakes. On the other hand, the combined effects of episodic stagnation of infiltrating precipitation in the unsaturated zone and the oxidizing character of this biologically-active environment promote the early dominance of Sr leaching from minerals such as K-feldspar and/or biotite and inheritance of relatively radiogenic Sr along upland groundwater recharge flowpaths. To the extent that strontium isotope signatures are maintained by groundwaters derived from these different recharge flowpaths, strontium isotopes, together with water isotopes and chemistry, may provide a powerful means for discerning the relative contributions of different groundwater sources to streams and wetlands in this region.

The second important conclusion of this study is that relative contributions from reactive phases can change along flowpaths, even though mineral proportions do not apparently change. This fact should come as no surprise, but should suggest caution to those who would attempt to oversimplify nature. A variety of factors such as relative mineral reactivities and the effects of secondary mineral formation need to be considered. At the very least, reaction path models that attempt to simulate the chemical evolution along groundwater flowpaths must be able to incorporate a changing reaction assemblage in the calculations, and environmental factors other than the calculated state of saturation must be considered.

Acknowledgments—The authors are grateful to the Northern Temperate Lakes/Long-Term Ecological Research project for establishing the network of wells on which this study is based, and to Galen Kenoyer for developing some of the original ideas about groundwater chemical evolution at this site. Logistical field support was provided by the Center for Limnology, Trout Lake Biological Station. This paper benefited substantially from discussions with Carl Bowser, Blair Jones, and Alex Blum, from especially thoughtful reviews by Alan Stueber and Berry Lyons, and from additional comments by two anonymous reviewers.

Editorial handling: J. Edmond

REFERENCES

- Aberg G., Jacks G., and Hamilton P. J. (1989) Weathering rates and $^{87}\text{Sr}/^{86}\text{Sr}$ ratios: an isotopic approach. *J. Hydrol.* **109**, 65–78.
- Attig J., Jr. (1985) Pleistocene geology of Vilas County, Wisconsin. Info. Circ. 50, Wis. Geol. Nat. Hist. Surv., Madison, 32 pp.
- Allen R. C. and Barret L. P. (1915) Contributions to the Precambrian geology of northern Michigan and Wisconsin. *Michigan Geol. and Biol. Surv. Publ.* **18**.
- Bailey S. W., Driscoll C. T., and Gaudette H. E. (1996) Calcium inputs and transport in a base-poor forest ecosystem as interpreted by Sr isotopes. *Water Resour. Res.* (in press).
- Bullen T. D., Kendall C., Krabbenhoft D. P., and Walker J. F. (1993) The natural variability of weathering input in a sandy silicate aquifer: evidence from Sr isotopes in groundwaters and experimental extracts. *EOS* **74**, 281. (abstr.)
- Bullen T. D., White A. F., Blum A. E., Schulz M. S. and Harden J. W. (1996) Chemical weathering of a soil chronosequence on granitoid alluvium: II. Mineralogic and isotopic constraints on the behavior of strontium. *Geochim. Cosmochim. Acta* (submitted).
- Burch T. E., Nagy K. L., and Lasaga A. C. (1993) Free energy dependence of albite dissolution kinetics at 80°C and pH 8.8. *Chem. Geol.* **105**, 137–162.
- Chaudhuri S., Broedel V., and Clauer N. (1983) Strontium isotopic evolution of oil-field waters from carbonate reservoir rocks in Bindley field, central Kansas, U.S.A. *Geochim. Cosmochim. Acta* **51**, 45–53.
- Cleaves E. T., Godfrey A. E., and Bricker O. P. (1970) Geochemical balance of a small watershed and its geomorphic implications. *Geol. Soc. Amer. Bull.* **81**, 3015–3032.
- Dincer T. (1968) The use of oxygen 18 and deuterium concentrations in the water balance of lakes. *Water Resour. Res.* **4**, 1289–1306.
- Elder J. F., Krabbenhoft D. P., and Walker J. F. (1992) Water, energy and biogeochemical budgets (WEBB) program: data availability and research at the Northern Temperate Lakes Site, Wisconsin. U.S.G.S. Open-File Report, 92–48.
- Faure G. (1986) *Principles of Isotope Geology* (2nd Ed.). Wiley.
- Fisher R. S. and Stueber A. M. (1976) Strontium isotopes in selected streams within the Susquehanna River basin. *Water Resour. Res.* **12**, 1061–1068.
- Garrels R. M. and Mackenzie F. T. (1967) Origin of the chemical compositions of some springs and lakes. In *Equilibrium Concepts in Natural Water Systems* (ed. R. F. Gould), pp. 222–242. ACS.
- Gosz J. R. and Moore D. I. (1989) Strontium isotope studies of atmospheric inputs to forested watersheds in New Mexico. *Biogeochem.* **8**, 115–134.
- Graustein W. C. (1990) $^{87}\text{Sr}/^{86}\text{Sr}$ ratios measure the sources and flow of strontium in terrestrial ecosystems. In *Stable Isotopes in Ecological Research* (ed. P. W. Rundell et al.), pp. 491–512. Springer-Verlag.
- Graustein W. C. and Armstrong R. L. (1983) The use of strontium-87/strontium-86 ratios to measure atmospheric transport into forested watersheds. *Science* **219**, 289–292.
- Harden J. W. (1987) Soils developed in granitic alluvium near Merced, California. U.S. Geol. Surv. Bull. 1590-A.
- Jacks G., Aberg G., and Hamilton P. J. (1989) Calcium budgets for catchments as interpreted by strontium isotopes. *Nordic Hydrol.* **20**, 85–96.
- Johnson T. M. and DePaolo D. J. (1994) Interpretation of isotopic data in groundwater-rock systems: model development and application to Sr isotope data from Yucca Mountain. *Water Resour. Res.* **30**, 1571–1587.
- Kenoyer G. J. and Anderson M. P. (1989) Groundwater's dynamic role in regulating acidity and chemistry in a precipitation-dominated lake. *J. Hydrol.* **109**, 287–306.
- Kenoyer G. J. and Bowser C. J. (1992a) Groundwater chemical evolution in a sandy silicate aquifer in northern Wisconsin, I. Patterns and rates of change. *Water Resour. Res.* **28**, 579–589.
- Kenoyer G. J. and Bowser C. J. (1992b) Groundwater chemical evolution in a sandy silicate aquifer in northern Wisconsin, II. Reaction modeling. *Water Resour. Res.* **28**, 591–600.
- Kharaka Y. K., Gunter W. D., Aggarwal P. K., Perkins E. H., and DeBrall J. D. (1988) SOLMINEQ.88: a computer program for geochemical modeling of water-rock interactions. USGS Water Resour. Invest. Rep. 88–4227.
- Krabbenhoft D. P., Bowser C. J., Anderson M. P., and Valley J. W. (1990) Estimating groundwater exchange with lakes. I. The stable isotope mass balance method. *Water Resour. Res.* **26**, 2445–2453.
- Krabbenhoft D. P., Bullen T. D., and Kendall C. (1992) Isotopic indicators of groundwater flow paths in a northern Wisconsin aquifer. *Eos* **73**, 190 (abstr.).
- Krabbenhoft D. P., Bowser C. J., Kendall C., and Gat J. (1994) Use of oxygen-18 and deuterium to assess the hydrology of groundwater-lake systems. In *Environmental Chemistry of Lakes and Reservoirs* (ed. L. Baker); *ACS Adv. Chem. Ser.* **237**, 67–90.
- Krabbenhoft D. P., Kendall C., and Bullen T. D. (1996) Delineation of groundwater flowpaths in a sandy silicate aquifer: a comparison of results from isotopic and numerical modeling studies. *Water Resources Res.* (submitted).
- Miller E. K., Blum J. D., and Friedland A. J. (1993) Determination of soil exchangeable-cation loss and weathering rates using Sr isotopes. *Nature* **362**, 438–441.

- Nesbit H. W. and Young G. M. (1984) Prediction of some weathering trends of plutonic and volcanic rocks based on thermodynamic and kinetic considerations. *Geochim. Cosmochim. Acta* **48**, 1523–1534.
- Stueber A. M., Walter L. M., Huston T. J., and Pushkar P. (1992) Formation waters from Mississippian-Pennsylvanian reservoirs, Illinois Basin, USA: chemical and isotopic constraints on evolution and migration. *Geochim. Cosmochim. Acta* **57**, 763–784.
- Turner J. V., Allison G. B., and Holmes J. W. (1984) The water balance of a small lake using stable isotopes and tritium. *J. Hydrol.* **70**, 199–220.
- Velbel M. A. (1985) Geochemical mass balances and weathering rates in forested watersheds of the southern Blue Ridge. *Amer. J. Sci.* **285**, 904–930.
- Wadleigh M. A., Veizer J., and Brooks C. (1985) Strontium and its isotopes in Canadian rivers: fluxes and global implications. *Geochim. Cosmochim. Acta* **49**, 1727–1736.
- Walker J. F., Krabbenhoft D. P., Kendall C., and Bullen T. D. (1992) Investigating streamflow generation in a small forested stream in Wisconsin using isotopic techniques. *EOS* **73**, 187. (abstr)
- White A. F. and Yee A. (1985) Aqueous oxidation-reduction kinetics associated with coupled electron-cation transfer from iron containing silicates. *Geochim. Cosmochim. Acta* **49**, 1263–1275.
- White A. F., Blum A. E., Schulz M. S., Bullen T. D., Harden J. W., and Peterson M. L. (1996) Chemical weathering of a soil chronosequence on granitoid alluvium: I. Reaction rates based on changes in soil mineralogy. *Geochim. Cosmochim. Acta* (submitted).
- Zhang H., Bloom P. R., and Nater E. A. (1993) Change in surface area and dissolution rates during hornblende dissolution at pH 4.0. *Geochim. Cosmochim. Acta* **57**, 1681–1689.